ce/papers Proceedings in civil engineering

Ernst & Sohn A Wiley Brand

ORIGINAL ARTICLE

EUROSTRUCT

Long-term validation of virtual sensing of a railway bridge with ballasted superstructure

Steven Robert Lorenzen[1] | Hagen Berthold[1] | Max Johannes Alois Fritzsche[1]| Maximilian Michael Rupp[1] | Henrik Riedel[1] | Eftychia Apostolidi[1] | Jens Schneider[1]

Correspondence

Steven R. Lorenzen
Technische Universität Darmstadt
Institute for Structural Mechanics and Design
Franziska-Braun-Straße 3
64287 Darmstadt
Email: lorenzen@ismd.tu-darmstadt.de

[1] Technical University of Darmstadt, Darmstadt, Germany

Abstract

Railway bridges have a long lifespan, which is challenged by the constant development of vehicles leading to increased loads that they were not originally designed for. To ensure the longest possible use of existing structures, a sensor-based structural health monitoring system can make a significant contribution. However, due to economic reasons and the inaccessibility of many points of interest, sensors cannot be installed everywhere. Therefore, in most cases, only a few sensors are available at a few points of interest, and methods that aim to reconstruct structural responses at unmeasured points from these measurements are referred to as virtual sensing. In this paper, we have analyzed 19,075 passages recorded on a steel trough bridge with a ballast superstructure and a span of 16.4 m, together with weather data. Our findings show that the influence of train type and speed has a significantly higher impact on the results than environmental factors. The investigation revealed that the model-based analysis produced similar results to the data-driven analysis concerning acceleration signals. However, when analyzing strain signals, the two approaches yielded distinctly different results.

Keywords

virtual sensing, railway bridges, long-term monitoring, field test, ballasted superstructure, response estimation, response reconstruction

1 Introduction

All over the world, the assessment of bridge structures is becoming increasingly important due to aging infrastructure and increasing traffic loads. To ensure the longest possible service life of bridges with sufficient safety against fatigue failure of all components, it is necessary to measure strains under real operating conditions instead of relying on load models from a standard [1,2]. Since many points of interest are not at all or poorly accessible, methods are desirable to determine the structural responses or quantities of interest over the entire structure, based on a few discretely measured points. These methods are referred to as virtual sensing or response estimation/reconstruction [1–7]. Virtual sensors generate signals by analysing the signals of physical sensors in combination with a process model [5, 11]. Virtual sensing techniques can be categorized as analytical/model-based or empirical/data-driven [6]. .Model-based methods use a structural dynamics model of the structure, usually a finite element (FE) model, to determine the quantities of interest from the signals of the physical sensors, while data-driven methods require at least a short-term measurement at the location of the virtual sensor [3,7]

To the best of our knowledge, there are only two studies for the validation of virtual sensing on railway bridges [7,12]. In the first study, the railway bridge KW51 with a ballast superstructure and a length of 115 m was investigated, and virtual sensing was implemented by using a method to determine the train loads. In the second investigation, a multi-span railway bridge with open deck and continuous girders was considered. The instrumented span had a length of 22 m. The modal expansion of FE-modes and the data-driven approach of Proper Orthogonal Decomposition (POD) mode expansion were validated. Both publications do not include long-term investigations. Therefore, we aim to contribute to filling two gaps: first, the investigation of short span bridges with ballasted superstructures, and second, the implementation of long-term investigations using virtual sensing. The first point is particularly important for Germany, as about 95% of railway bridges are shorter than 30 m [9].

2 Methods

2.1 Virtual sensing via mode expansion

It is well-established that degrees of freedom in FE models can be reduced through modal decorrelation, which enables a relationship to be established between retained and omitted degrees of freedom [10]. This relationship can be useful for virtual sensing, but it only applies to linear and time-invariant systems. Structural Modification Theory,

https://doi.org/10.1002/cepa.2126

however, proves that the system responses of a perturbed system with a modified mass, stiffness, or damping matrix still lie in the space spanned by the eigenmodes of the unperturbed system [11].

In a laboratory experiment presented in [5], Tarpø et al. demonstrated that virtual sensing can be achieved through the eigenmodes of a linear FE model, at least for subsystems of a mechanically nonlinear system. As strains and displacements in bridge structures during operation are typically small, the structural response can be approximated based on the eigenmodes of the linear bridge model, even though the overall system behaviour (including the bridge, superstructure, and vehicle-structure interaction effects) is mechanically nonlinear.

POD offers the possibility to extract modes from the discrete measurements, also called snapshots of the system, without the need to know the underlying dynamics of the system. These modes can also be used to approximate measurements in a low-rank subspace to enable virtual sensing. A detailed description of POD and the model reduction based on it can be found in [12].

The calculation of the quantities of interest at the points of the virtual sensors can be summarised as follows:

$$\boldsymbol{Y} = \begin{Bmatrix} \boldsymbol{y}_\mathrm{m} \\ \boldsymbol{y}_\mathrm{u} \end{Bmatrix} \approx \boldsymbol{\theta q} = \begin{bmatrix} \boldsymbol{\theta}_\mathrm{m} \\ \boldsymbol{\theta}_\mathrm{u} \end{bmatrix} \boldsymbol{q} \quad (1)$$

$$\widehat{\boldsymbol{Y}} = \begin{Bmatrix} \widehat{\boldsymbol{y}}_\mathrm{m} \\ \widehat{\boldsymbol{y}}_\mathrm{u} \end{Bmatrix} \approx \boldsymbol{\theta}\widehat{\boldsymbol{q}} = \boldsymbol{\theta}\boldsymbol{\theta}_\mathrm{m}^{+}\boldsymbol{y}_\mathrm{m} \quad (2)$$

$\boldsymbol{Y} \in \mathbb{R}^{N\times t}$ is the response matrix containing the quantity of interest for all N degrees of freedom of the FE model or at all N points of the POD-modes gathered from a short-time measurement, where t is the number of samples (time steps). The response matrix $\boldsymbol{Y}$ is divided into the measured degrees of freedom $\boldsymbol{y}_\mathrm{m} \in \mathbb{R}^{a\times t}$ and the unmeasured degrees of freedom $\boldsymbol{y}_\mathrm{u} \in \mathbb{R}^{(N-a)\times t}$, where a is the number of measurements (sensor channels). $\boldsymbol{\theta} \in \mathbb{R}^{N\times M}$ is the mode matrix where M is the number of modes considered. The mode matrix is also divided into the measured and unmeasured degrees of freedom $\boldsymbol{\theta}_\mathrm{m} \in \mathbb{R}^{a\times M}$ and $\boldsymbol{\theta}_\mathrm{u} \in \mathbb{R}^{(N-a)\times M}$, respectively. $\boldsymbol{q} \in \mathbb{R}^{M\times t}$ contains the weights of the modes used to approximate the structural response. $\widehat{\boldsymbol{Y}}$ is the approximation based on the least squares estimation of the weights $\widehat{\boldsymbol{q}}$. $\boldsymbol{\theta}_\mathrm{m}^{+}$ is the Moore-Penrose pseudoinverse of $\boldsymbol{\theta}_\mathrm{m}$. To obtain meaningful results and to avoid overfitting, an overdetermined system of equations should be constructed, i.e., the number of physical sensors should be greater than the number of modes considered.

2.2 Data acquisition

We collected data from a single-span steel trough bridge (Figure 1) located on a frequently used long-distance route in Germany. The bridge has a free span of 16.4 m and a total length of 18.4 m. During the recording phase, we installed 9 uniaxial accelerometers, 8 uniaxial strain gauges, and 4 type K thermocouples along the two main girders of the bridge. Additionally, two pairs of rosette strain gauges were installed on the tracks at a distance of 14.40 m to record the axles of trains (Figure 2).

For this contribution, we analysed 19,075 passages of the bridge from three different time intervals: 28 October 2021 to 17 January 2022, 9 February to 28 March 2022, and 26 July to 7 September 2022. In addition to the data recorded at the bridge, data from a weather station located 1.3 kilometers away was also utilized (Figure 3).

Figure 1 Examined single-span steel trough bridge.

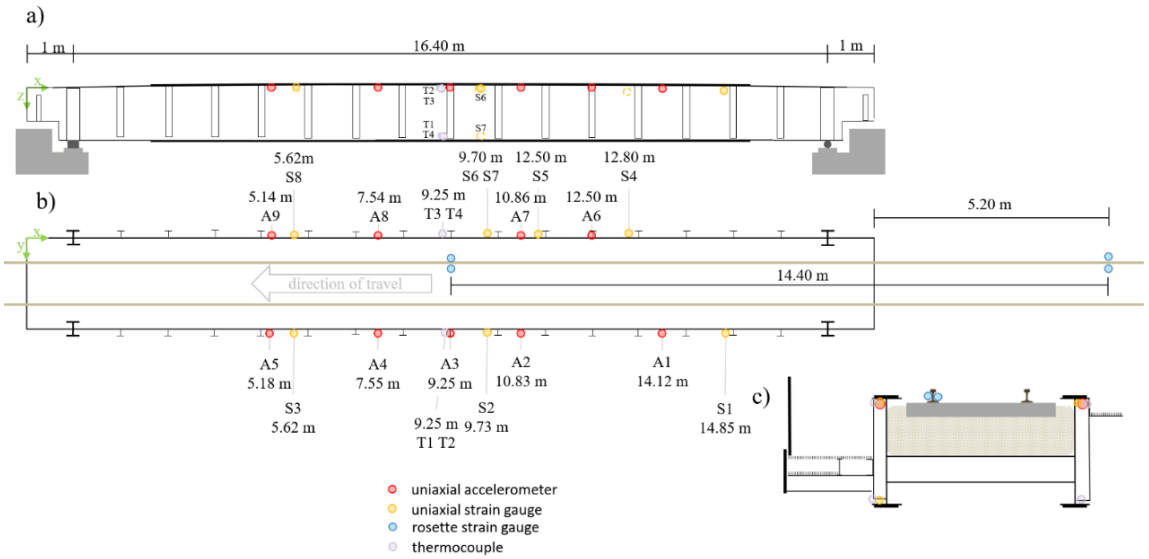

Figure 2 Sensor setup with labels and x-coordinate of the sensors: a) side view b) top view c) cross-section

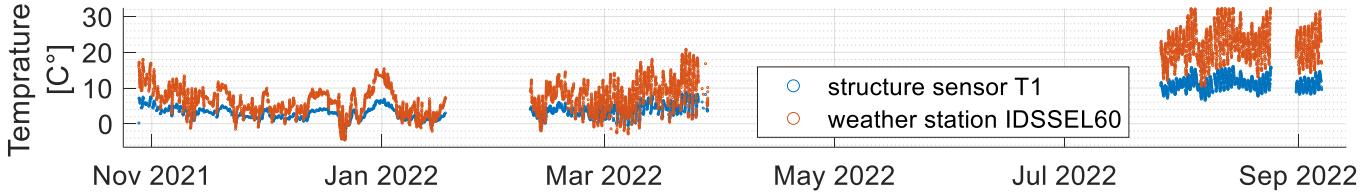

Figure 3 Comparison of temperature measurements between the bridge and the weather station located 1.3 kilometres away during the three investigated time intervals.

2.3 Considered modes

We created an FE model of the bridge using the commercial software SOFiSTiK with 585,084 degrees of freedom. The main load-bearing structure was modelled with surface elements, while the attached walkway and handrail were modelled with beam elements. The ballast was treated as an additional mass, and its stiffness contribution was neglected. However, we approximated the partial clamping effects from the ballast superstructure using springs at the ends of the top flanges of the main girders. For this article, we only considered the first two bending and torsional eigenmodes, as shown in Figure 4.

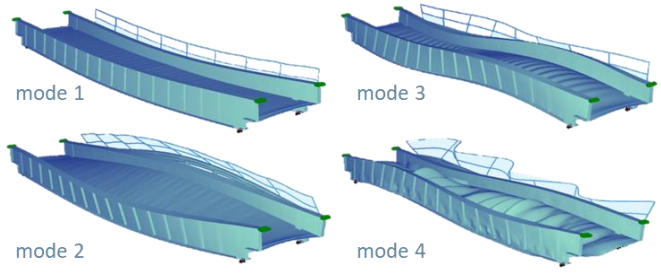

Figure 4 Considered modes of the FE model (view from the opposite side compared to the Fig. 1).

In contrast to the eigenmodes of the FE model, the POD-modes are dependent on the excitation. For this investigation, we randomly selected one passage and determined the POD-modes for the strain and acceleration signals. These modes were then used to evaluate all other passages in this study. A more reasonable selection of the POD-modes should be made in future studies.

2.4 Scoring of the estimates

To compare the numerous passages, an error metric is required to evaluate the results of virtual sensing. We chose the coefficient of determination as the error metric because it depends on amplitude differences unlike the widely used Time Response Assurance Criterion (TRAC) [4]. The coefficient of determination R^2, as given in Equation (3), compares the physical sensor measurement with the result of the virtual sensor. It quantifies the difference between the two measurements and determines the accuracy and reliability of the virtual sensor in predicting the response of the structure.

$$R^2 = 1 - \frac{\mathrm{E}[(y_i - \hat{y}_i)^2]}{\mathrm{Var}(y_i)} \qquad (3)$$

Where $y_i \in \mathbb{R}^t$ is the signal of the i-th sensor and $\hat{y}_i$ is the estimation.

To give an impression of the relationship between the coefficient of determination and the goodness of the estimate, the signals and their estimates and the associated residual (y_i-$\hat{y}_i$) are given below for 4 different coefficients of determination.

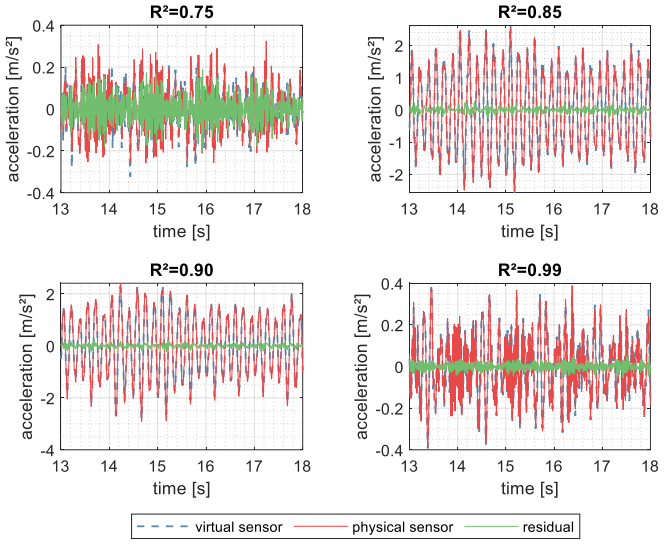

Figure 5 Examples to illustrate the goodness of the virtual sensors quantified using the coefficient of determination. Note the different scaling of the y-axes.

3 Results and discussion

This section presents evaluations of the measurements described in Section 2.

3.1 Amplitude dependent frequencies

The behaviour of railway ballast is highly non-linear and is dependent on both the load and environmental conditions such as temperature and humidity [13]. In a previous study by Reiterer and Firus [14], the shift of the resonance frequency of a steel bridge with ballast superstructure was determined. Another study by Lorenzen et al. [15] analysed free decay phases of the same bridge and plotted the frequency of the first bending mode against the measured maximum displacements during the free decay. This analysis showed a clear functional relationship between the maximum amplitude of the free decay and the frequency of the first bending mode [15]. Since displacement measurements were not available for the investigations in this paper, we used the maximum strain in the centre of the span, which is strongly correlated with the displacement for the free vibration. The decay phase signals were used to perform the Stochastic Subspace Identification (SSI) automatically using the code from [16]. The time points when the trains left the bridge were determined by analysing the signals from the rosette strain gauges on the tracks. The analysis results show that the amplitude-dependent frequency shift is affine to the frequency shift of

the bridge observed in [15] (Figure 6).

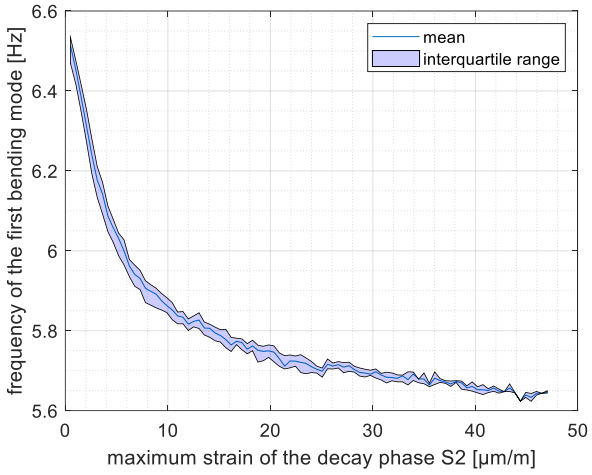

Figure 6 First bending frequency determined by SSI from the decay phases as a function of the maximum absolute values of the strain in the centre of the bridge span.

3.2 Virtual acceleration sensing

For the virtual sensing methods described in Section 2.1, it is possible to vary the number of physical sensors k and the number of considered modes M. For k physical sensors, there are $\binom{a}{k}$ combinations. All sensors not used as physical sensors are defined as virtual sensors. For each of the 19,075 passages, the coefficient of determination for all $\binom{a}{k}$ combinations were calculated. For each combination, the mean value of the coefficient of determination was determined over all passages.

Figure 7 and Figure 8 show the mean values of the coefficients of determination for the best and worst of the $\binom{a}{k}$ combinations, considering the FE-modes and the POD-modes, respectively. Since the values of the coefficient of determination for bad combinations can approach infinity, mean values smaller than 0 were not shown for good visualization purposes. Mean values below 0 are indicated in white with a grey edge. For the case that $k = a - 1$ there is only one combination so that the minimum value is equal to the maximum value.

The analysis of acceleration signals indicates that the use of FE modes and POD-modes yields similar results. Even with a few physical sensors and modes, good results can be achieved. However, the choice of combination has a significant impact on the outcome, as demonstrated by the large differences between the minimum and maximum values. Increasing the number of physical sensors reduces the dependence on the chosen combination.

To analyse the effects of environmental factors, the data from the weather station were compared to the coefficients of determination of virtual sensors obtained by using $k = a - 1$ physical sensors and considering $M = 4$ modes. Outliers were identified for each sensor individually by removing coefficients of determination that were more than 1.5 interquartile ranges above the upper quartile or below the lower quartile. The Pearson correlation coefficient was then calculated with a significance level of $\alpha = 0.001$ for the remaining dataset. Table 1 summarises the results, which indicate a weak or no correlation between environmental factors and the coefficient of determination for all sensors. The signs of the correlation are the same for one environmental variable for all sensors. The use of POD-modes results in a slightly higher correlation compared to the use of FE-modes.

Table 1 Pearson correlation coefficients between the environmental variables and the coefficient of determination using $k = a - 1$ physical sensors and $M = 4$ considered modes and a significance level of $\alpha = 0.001$. n.s.: not significant

	temperature		relative humidity		wind speed		wind gust		precipitation rate		precipitation accumulation	
sensor	FE	POD	FE	POD	FE	POD	FE	POD	FE	POD	FE	POD
A1	n.s	-0.06	0.05	0.11	-0.05	-0.08	-0.05	-0.08	ns.	n.s.	n.s.	n.s.
A2	n.s	-0.11	0.04	0.12	-0.05	-0.07	-0.05	-0.07	ns.	n.s.	n.s.	n.s.
A3	n.s	-0.10	0.07	0.12	-0.07	-0.06	-0.07	-0.06	ns.	n.s.	n.s.	n.s.
A4	-0.08	-0.10	0.08	0.10	-0.06	-0.06	-0.06	-0.06	ns.	n.s.	n.s.	n.s.
A5	n.s	-0.08	0.05	0.10	-0.06	-0.06	-0.06	-0.06	ns.	n.s.	n.s.	n.s.
A6	-0.04	-0.15	0.08	0.15	-0.06	-0.06	-0.06	-0.06	ns.	n.s.	n.s.	0.03
A7	-0.03	-0.14	0.07	0.16	-0.06	-0.08	-0.06	-0.08	ns.	n.s.	n.s.	n.s.
A8	-0.07	-0.07	0.08	0.09	-0.04	-0.05	-0.04	-0.05	ns.	n.s.	n.s.	n.s.
A9	-0.06	-0.09	0.08	0.08	-0.05	-0.04	-0.05	-0.04	ns.	n.s.	n.s.	n.s.

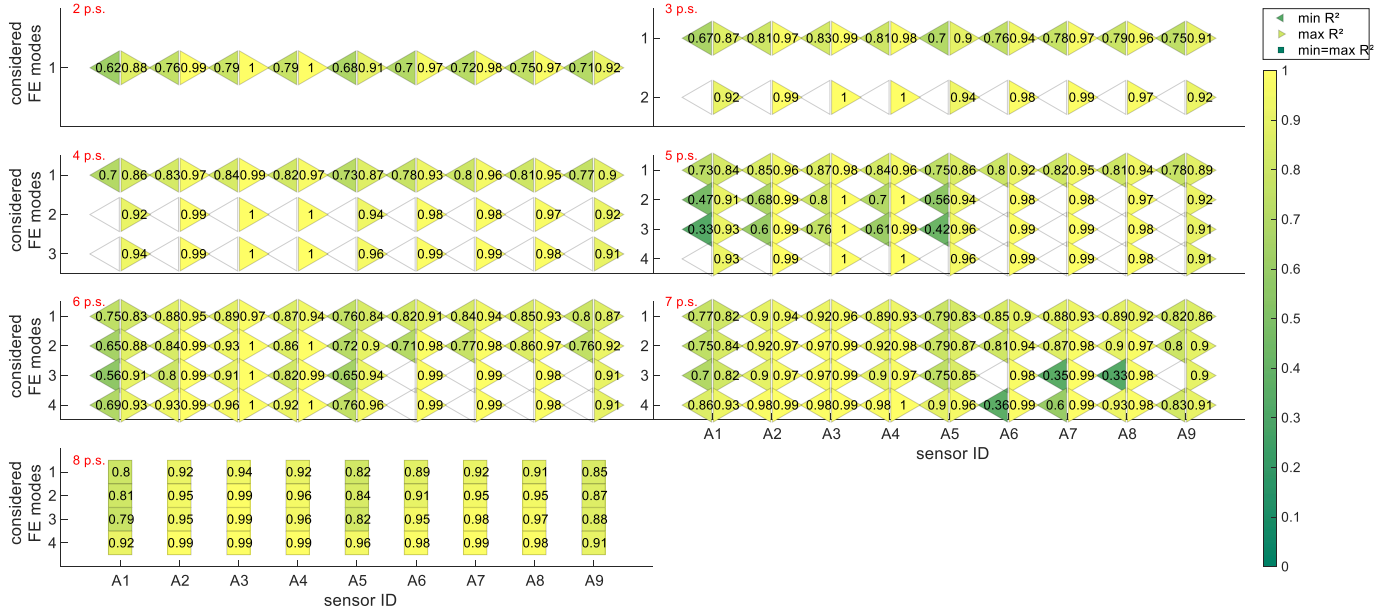

Figure 7 Summary of the minimum and maximum values of the coefficients of determination of the acceleration sensors A1 to A9 as a function of the FE-modes used and the number of physical sensors (p.s.).

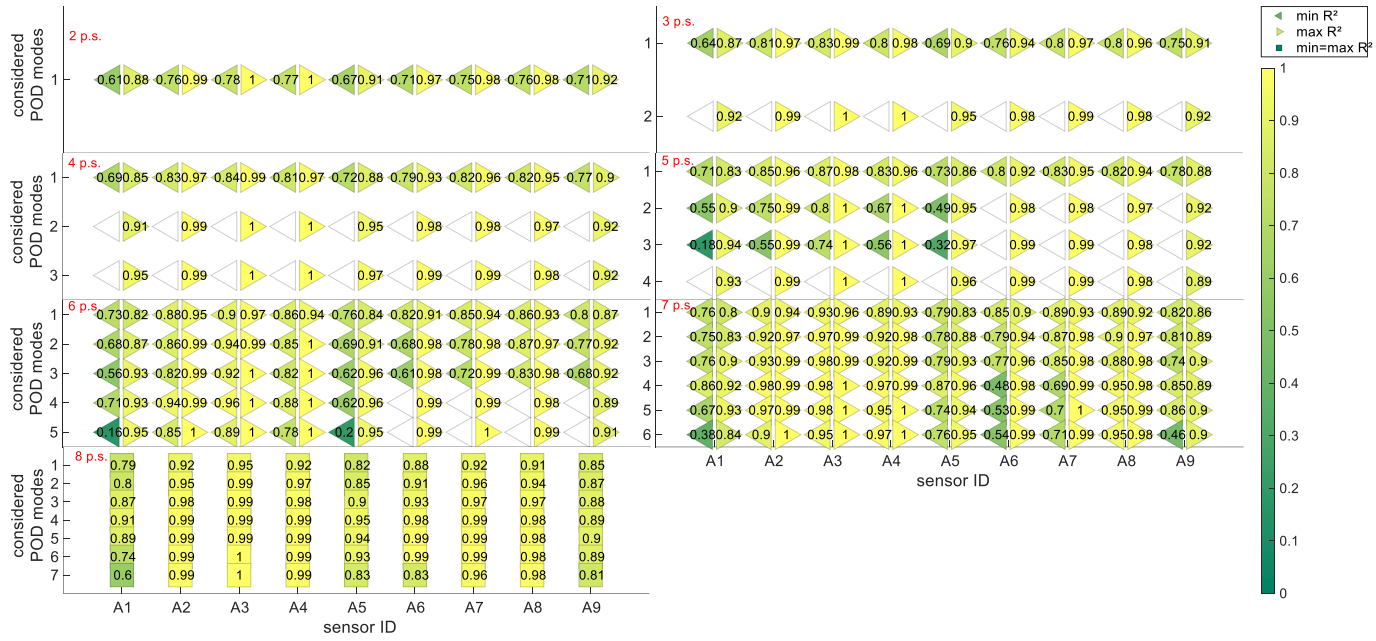

Figure 8 Summary of the minimum and maximum values of the coefficients of determination of the acceleration sensors A1 to A9 as a function of the POD-modes used and the number of physical sensors (p.s.).

To investigate the influence of changes in operation due to different trains and train speeds, the trains were classified using measurements from the rosette strain gauges on the rails and the average speed per passage was determined. The coefficient of determination for $k = a - 1$ physical sensors and $M = 4$ was then plotted against the speed for each sensor, in the scope of this paper they are only presented for one train type (Figure 9). There is a clear functional relationship between the coefficient of determination and the speed. This is because in the resonance case the structural response is dominated by one degree of freedom. In this case it is the first bending mode (Figure 4, mode 1).

3.3 Virtual strain sensing

This subsection applies the same analyses as the previous section to the strain measurements. However, unlike the accelerations, the choice of FE-modes or POD-modes has an impact (Figure 10-12). The use of POD-modes leads to better results than the use of FE-modes. However, with the notable exception of the S7 sensor, which cannot be reconstructed at all with the POD-modes used.

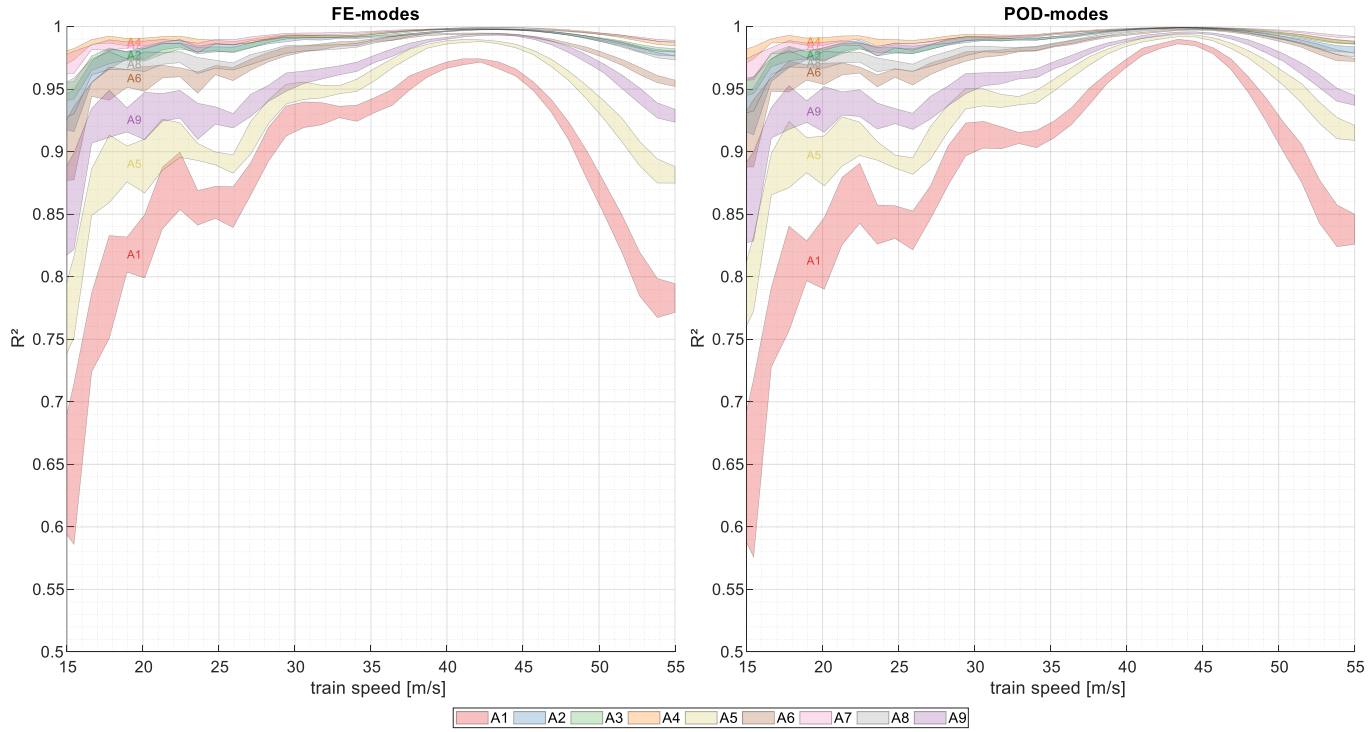

Figure 9 Interquartile range of the coefficients of determination against speed of the train for each acceleration sensor for one train type, separated into FE-modes and POD-modes. Note the different scaling of the y-axes.

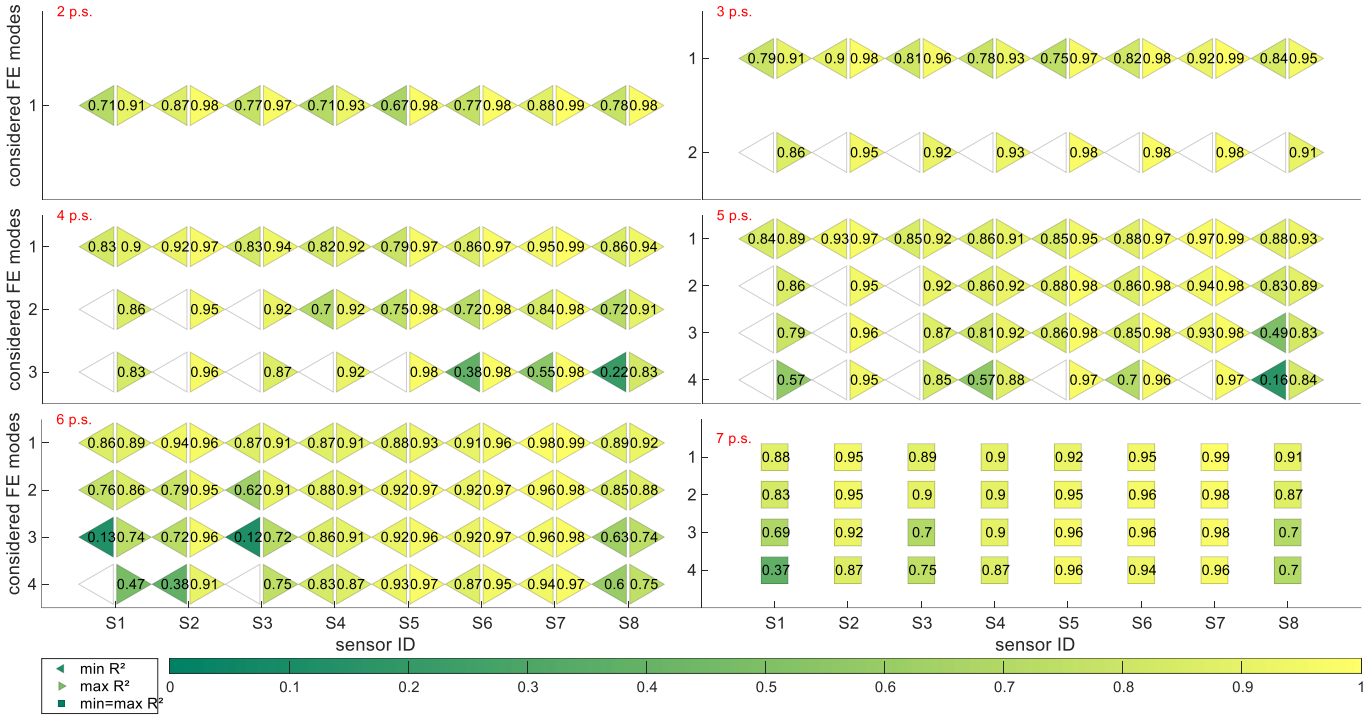

Figure 10 Summary of the minimum and maximum values of the coefficients of determination of the strain sensors S1 to S8 as a function of the FE-modes used and the number of physical sensors (p.s.).

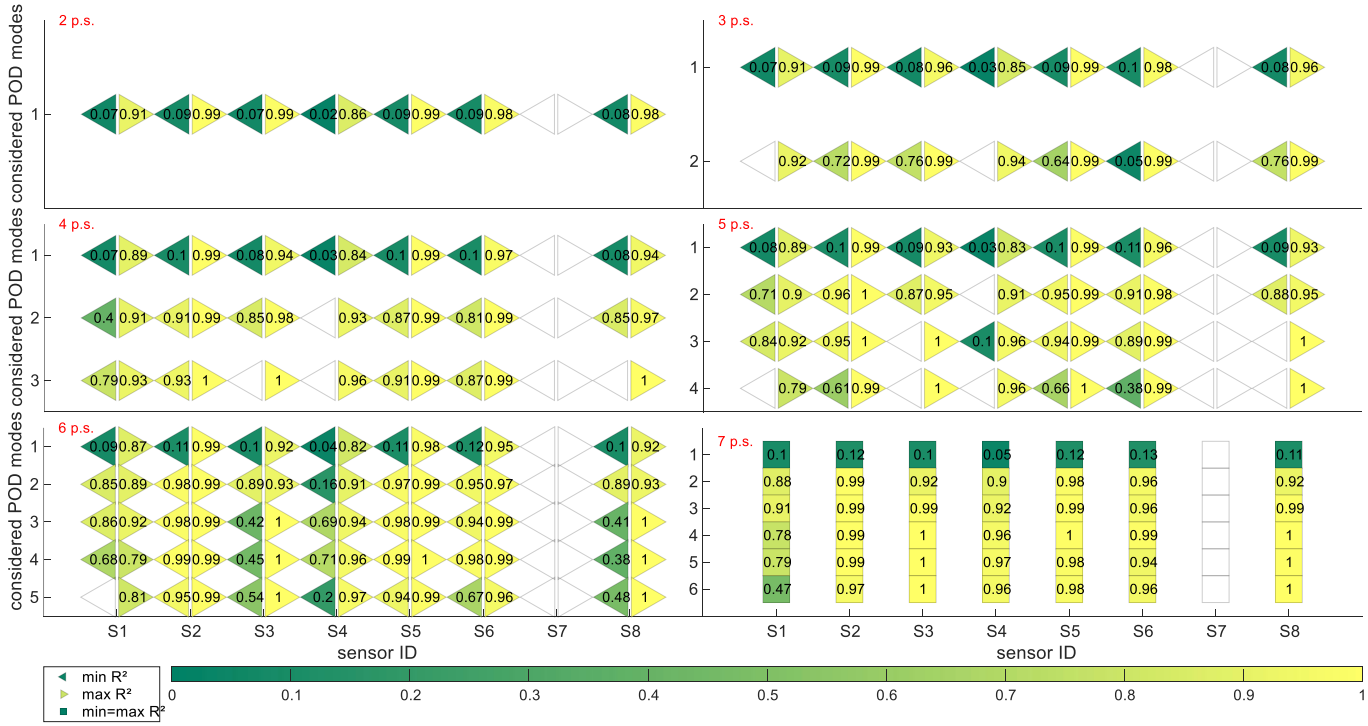

Figure 11 Summary of the minimum and maximum values of the coefficients of determination of the strain sensors S1 to S8 as a function of the POD-modes used and the number of physical sensors (p.s.).

The investigation of the environmental influences shows a moderate to strong correlation to temperature and a small to moderate correlation to humidity for the strains for both POD-modes and FE-modes. There is little or no correlation with the other variables. Table 2 summarises the results. To get an impression of the changes as a function of temperature, Figure 13 shows the coefficient of determination for the individual sensor as a function of temperature separately for FE-modes and POD-modes. For the investigated temperature range, the estimates of the virtual sensors remain of similar quality.

The investigation of the influence of train type and speed is interesting. Here, the FE-modes show an analogous behaviour to the accelerations. With the POD-modes, however, the coefficient of determination decreases in the resonance range (approximately between 40 m/s and

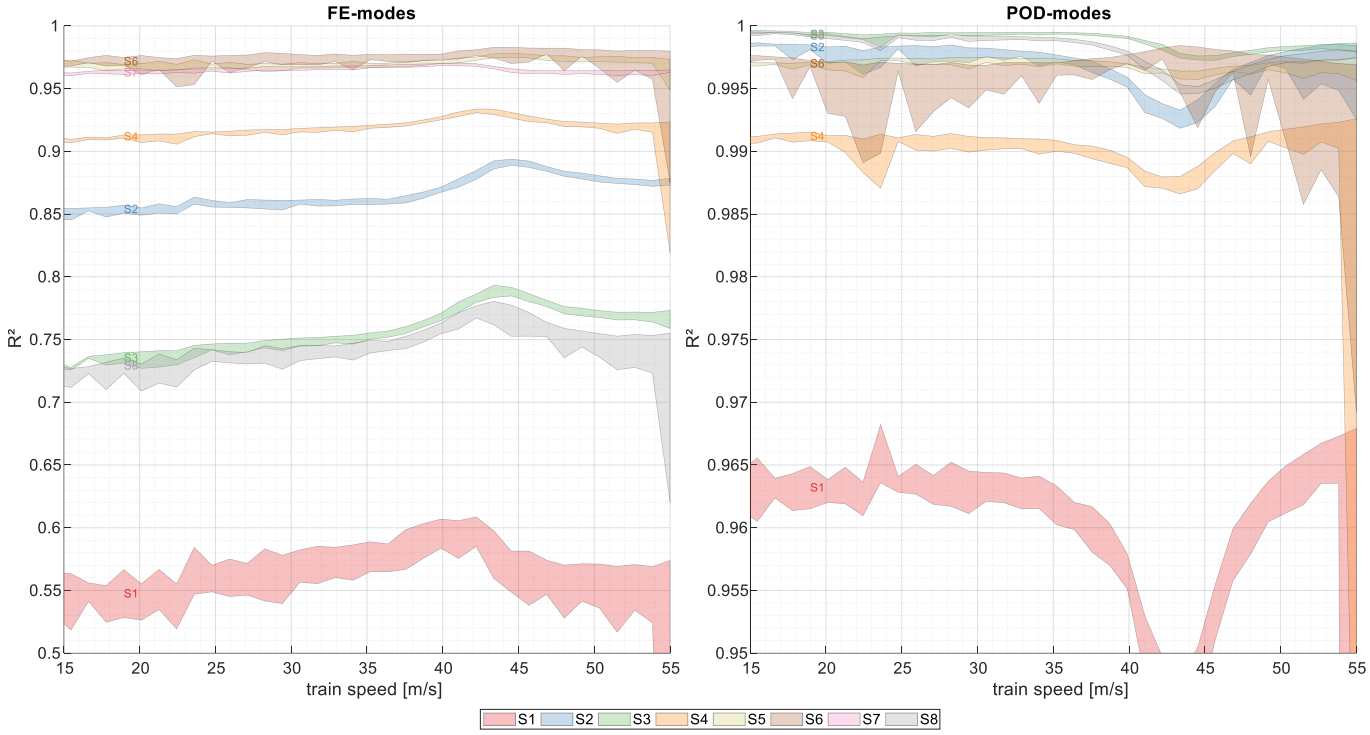

Figure 12 Interquartile range of the coefficients of determination against speed of the train for each strain sensor for one train type, separated into FE-modes and POD-modes. Note the different scaling of the y-axes.

45 m/s), which is exactly the opposite of the FE-modes (Figure 12).

Table 2 Pearson correlation coefficients between the environmental variables and the coefficient of determination using $k = a - 1$ physical sensors and $M = 4$ considered modes and a significance level of $\alpha = 0.001$. n.s.: not significant

	temperature		relative humidity		wind speed		wind gust		precipitation rate		precipitation accumulation	
sensor	FE	POD	FE	POD	FE	POD	FE	POD	FE	POD	FE	POD
S1	-0.14	0.05	0.07	-0.09	0.10	0.11	0.1	0.11	0.03	n.s.	0.03	n.s
S2	0.12	-0.37	-0.19	0.25	0.10	0.04	0.09	0.05	n.s.	0.04	n.s.	0.09
S3	-0.08	-0.27	n.s.	0.24	n.s.	-0.04	n.s.	-0.03	n.s.	n.s.	n.s.	0.05
S4	-0.21	-0.35	0.10	0.24	n.s.	0.06	n.s.	0.07	n.s.	0.03	n.s.	0.1
S5	0.64	-0.49	-0.47	0.30	0.20	0.11	0.19	0.13	n.s.	0.06	n.s.	0.14
S6	-0.81	-0.69	0.46	0.43	-0.07	0.08	-0.06	0.1	0.04	0.09	0.08	0.16
S7	-0.62		0.46		-0.14		-0.12		n.s.		0.04	
S8	-0.29	-0.23	0.14	0.20	0.10	n.s.	0.1	n.s.	n.s.	n.s.	0.06	0.04

4 Conclusion

In the field of virtual sensing on railway bridges, no studies have been published on short span bridges with ballast superstructure, nor have any long-term studies been conducted. To address this gap, we analysed over 19,000 passages on a steel trough bridge with a span of 16.4 m. In addition to measurements on the bridge, we used data from a weather station located 1.3 kilometres away to assess the influence of environmental conditions. Specifically, we investigated acceleration and strain measurements. Overall, our analysis provided valuable insights into the behaviour of virtual sensors under varying environmental and operating conditions. The following key findings can be highlighted:

Accelerations:

1. Both FE-modes and POD-modes yield similar results, but the choice of sensor combination has a significant impact on the result.
2. Increasing the number of physical sensors reduces the dependence on the chosen sensor combination.
3. There is a clear functional relationship between the coefficient of determination and the train speed. The maximum of the coefficient of determination is reached at the resonance speed.
4. Environmental factors show weak or no correlation to the coefficient of determination for all sensors. The use of POD-modes results in a slightly higher correlation compared to FE-modes.

Strains:

1. The use of POD-modes leads to better results than FE-modes, except for sensor S7, which cannot be reconstructed with the used POD-modes.
2. Environmental influences show moderate to strong correlation to temperature and small to moderate correlation to humidity, but little to no correlation with other weather variables.
3. The estimates of virtual sensors remain of similar quality for the investigated temperature range.
4. The behaviour of virtual sensors with respect to train type and speed differs between FE-modes and POD-modes, with the former showing analogous behaviour to accelerations, while the latter showing a decrease of the coefficient of determination around the resonance speed.

Overall, the study showed that the greatest influence on the coefficient of determination is given by the train type and the speed, the effect is much greater than that of the environmental influences. These findings provide important insights into the performance of virtual sensors in railway systems and can inform the development of more robust and accurate virtual sensor systems in the future.

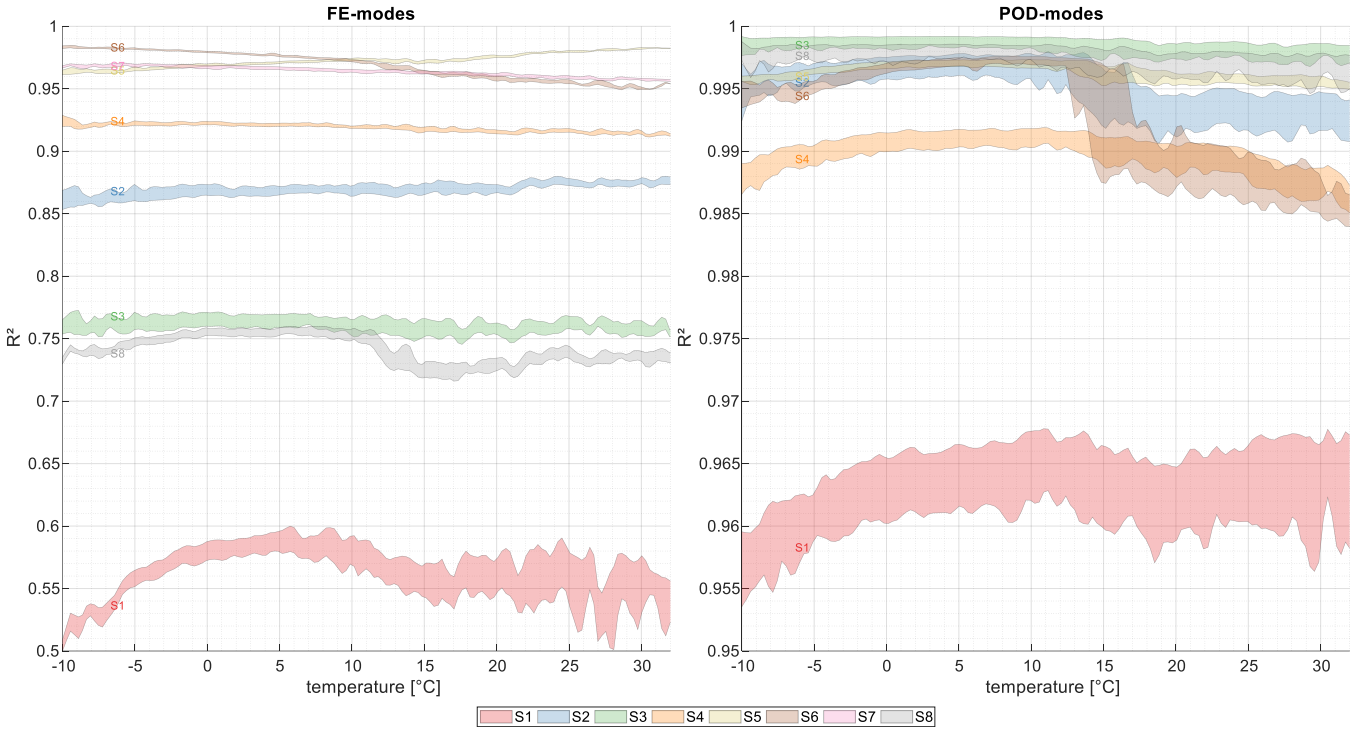

Figure 13 Interquartile range of the coefficients of determination of the outlier-cleaned data set versus temperature for each of the strain sensors, separated into FE-modes and POD-modes. Note the different scaling of the y-axes.

Acknowledgements

The authors would like to acknowledge the financial support of the research project ZEKISS ("Condition assessment of railroad bridges and vehicles with AI methods for the evaluation of sensor data and structural dynamic models"), funded by mFund (mFund, 2020) awarded by the Federal Ministry of Transport and Digital Infrastructure of Germany. Research in ZEKISS is carried out in collaboration with the German railway company DB Netz AG, the Wolfel Engineering GmbH and the GMG Ingenieurgesellschaft mbH (www.zekiss.de).

Gefördert durch:

Bundesministerium für Digitales und Verkehr

aufgrund eines Beschlusses des Deutschen Bundestages

References

[1] Maes, K., De Roeck, G., Lombaert, G., Cunha, A., Caetano, E., Ribeiro, P., & Müller, G. (2014, July). Response estimation in structural dynamics. In *Proceedings of the 9th International Conference on Structural Dynamics, EURODYN 2014* (Vol. 2014). EUROPEAN ASSOC STRUCTURAL DYNAMICS.

[2] Maes, K., Iliopoulos, A., Weijtjens, W., Devriendt, C., & Lombaert, G. (2016). Dynamic strain estimation for fatigue assessment of an offshore monopile wind turbine using filtering and modal expansion algorithms. *Mechanical Systems and Signal Processing*, *76*, 592-611

[3] Peng, Z., Dong, K., & Yin, H. (2019). A modal-based kalman filter approach and Osp method for structural response reconstruction. *Shock and Vibration*, *2019*.

[4] Liu, L., Kuo, S. M., & Zhou, M. (2009, March). Virtual sensing techniques and their applications. In *2009 International Conference on Networking, Sensing and Control* (pp. 31-36). IEEE.

[5] Tarpø, M., Friis, T., Georgakis, C., & Brincker, R. (2021). Full-field strain estimation of subsystems within time-varying and nonlinear systems using modal expansion. *Mechanical Systems and Signal Processing*, *153*, 107505.

[6] Kullaa, J. (2019). Bayesian virtual sensing in structural dynamics. *Mechanical Systems and Signal Processing*, *115*, 497-513.

[7] Maes, K., & Lombaert, G. (2021). Validation of virtual sensing for the fatigue assessment of steel railway bridges. In *Life-Cycle Civil Engineering: Innovation, Theory and Practice* (pp. 297-304). CRC Press.

[8] Azam, S. E., Didyk, M. M., Linzell, D., & Rageh, A. (2022). Experimental validation and numerical investigation of virtual strain sensing methods for steel railway bridges. *Journal of Sound and Vibration*, *537*, 117207.

[9] Geißler, K. (2014). *Handbuch Brückenbau: Entwurf, Konstruktion, Berechnung, Bewertung und Ertüchtigung*. John Wiley & Sons.

[10] Kammer, D. C. (1987). Test-analysis model development using an exact modal reduction. *International Journal of Analytical and Experimental Modal Analysis*, *2*(4), 174-179.

[11] Sestieri, A. (2000). Structural dynamic modification. *Sadhana*, *25*, 247-259.

[12] Brunton, S. L., & Kutz, J. N. (2019). *Data-driven science and engineering: Machine learning, dynamical systems, and control*. Cambridge University Press.

[13] Liu, J., Wang, P., Liu, G., Dai, J., Xiao, J., & Liu, H. (2021). Study of the characteristics of ballast bed resistance for different temperature and humidity conditions. *Construction and Building Materials*, *266*, 121115.

[14] Reiterer, M., & Firus, A. (2022). Dynamische Analyse der Zugüberfahrt bei Eisenbahnbrücken unter Berücksichtigung von nichtlinearen Effekten. *Beton- und Stahlbetonbau*, *117*(2), 90-98.

[15] Lorenzen, S. R., Berthold, H., Rupp, M., Schmeiser, L., Apostolidi, E., Schneider, J., ... & Rüppel, U. (2022). Deep learning based indirect monitoring to identify bridge natural frequencies using sensors on a passing train. In *Bridge Safety, Maintenance, Management, Life-Cycle, Resilience and Sustainability* (pp. 401-409). CRC Press.

[16] Cheynet, E. Operational Modal Analysis with Automated Ssi-Cov Algorithm, 2020. *URL https://zenodo. org/record/3774061*, *104*.